

Finite-size scaling of quasi-stationary-state temperature

Antonio Rodríguez ¹, Fernando D. Nobre,² and Constantino Tsallis ^{2,3,4}

¹*GISC, Departamento de Matemática Aplicada a la Ingeniería Aeroespacial, Universidad Politécnica de Madrid, Plaza Cardenal Cisneros s/n, 28040 Madrid, Spain*

²*Centro Brasileiro de Pesquisas Físicas and National Institute of Science and Technology for Complex Systems, Rua Dr. Xavier Sigaud 150, 22290-180 Rio de Janeiro, Brazil*

³*Santa Fe Institute, 1399 Hyde Park Road, Santa Fe, New Mexico 87501, USA*

⁴*Complexity Science Hub Vienna, Josefstädter Strasse 39, 1080 Vienna, Austria*



(Received 17 January 2022; accepted 18 March 2022; published 7 April 2022)

We numerically study, from first principles, the temperature T_{QSS} and duration t_{QSS} of the longstanding initial quasi-stationary state of the isolated d -dimensional classical inertial α -XY ferromagnet with two-body interactions decaying as $1/r_{ij}^\alpha$ ($\alpha \geq 0$). It is shown that this temperature T_{QSS} (defined proportional to the kinetic energy per particle) depends, for the long-range regime $0 \leq \alpha/d \leq 1$, on (α, d, U, N) with numerically negligible changes for dimensions $d = 1, 2, 3$, with U the energy per particle and N the number of particles. We verify the finite-size scaling $T_{\text{QSS}} - T_\infty \propto 1/N^\beta$ where $T_\infty \equiv 2U - 1$ for $U \lesssim U_c$, and β appears to depend sensibly only on α/d . Our numerical results indicate that neither the scaling with N of T_{QSS} nor that of t_{QSS} depend on U .

DOI: [10.1103/PhysRevE.105.044111](https://doi.org/10.1103/PhysRevE.105.044111)

I. INTRODUCTION

Nonequilibrium regimes appear frequently in nature, mostly in systems characterized by many-interacting particles, and are usually investigated through the tools of nonequilibrium statistical mechanics [1–4]. In some cases these regimes present intriguing behavior, such as a lifetime that increases with the total number of particles N , dependence on the initial conditions, irreversibility, and breakdown of ergodicity, the latter being associated with a noncommutative property involving two relevant limits, namely, the long-time ($t \rightarrow \infty$) and thermodynamic ($N \rightarrow \infty$) limits. Ergodicity represents a basic pillar for the application of Boltzmann-Gibbs (BG) statistical mechanics, supporting the use of standard equations describing the time evolution of these systems, and particularly, their approach to an equilibrium state; its breakdown indicates that some such equations may need modifications [5,6].

A model that exhibits some of the above-mentioned features is the so-called Hamiltonian mean-field (HMF) model [7], characterized by classical XY rotators coupled through infinite-range interactions, i.e., a limit where the mean-field approach becomes exact. The HMF model has been largely investigated in the literature (see, e.g., Refs. [7–18]), yielding many anomalous properties, such as long-living quasi-stationary states (QSSs), negative specific heat, and non-Maxwellian velocity probability distributions. Studying numerically the time evolution of the average kinetic temperature $T(t)$, one usually finds that this model exhibits two distinct states: a QSS, characterized by a kinetic temperature T_{QSS} , followed by a later state whose temperature T_{BG} ($T_{\text{BG}} > T_{\text{QSS}}$) coincides with the one predicted by BG

statistical mechanics. Intriguingly, the duration t_{QSS} of the first state increases with the total number of rotators N , so that considering the limit $N \rightarrow \infty$ first, the system would remain in the QSS, never reaching the later state with temperature T_{BG} , reflecting the above-mentioned ergodicity breakdown.

The QSSs that appear in the HMF model manifest another peculiarity, concerning the fact that they appear in a ferromagnetic phase, for values of the energy per particle below (but close) to the critical value ($U \lesssim U_c$), as a low-temperature extension of the high-temperature (paramagnetic) branch of the caloric curve. This curious phenomenon may be compared to metastable states commonly observed in supercooled liquids [19,20]. Moreover, these states correspond to a vanishing magnetization, independently from the initial conditions considered for the orientations of the rotators, which are observed for both maximal and minimal initial magnetizations. In the limit $N \rightarrow \infty$, one has that the associated kinetic temperature T_∞ is related to the energy per particle in a simple way [13–15],

$$T_\infty \equiv \lim_{N \rightarrow \infty} T_{\text{QSS}}(N) = 2U - 1. \quad (1.1)$$

In the present work we carry a detailed analysis of the above limit, extending the investigation to the whole long-range regime ($0 \leq \alpha/d \leq 1$) of the d -dimensional classical inertial α -XY ferromagnet with two-body interactions decaying as $1/r_{ij}^\alpha$ ($\alpha \geq 0$). In such a case, Eq. (1.1) will be shown to apply to typical values of (α, d, U) , and that the temperature T_∞ is approached through the following scaling with N :

$$T_{\text{QSS}}(N) - T_\infty \propto N^{-\beta}. \quad (1.2)$$

Our numerical study suggests that the exponent β does not depend on d for fixed α/d , presenting imperceptible changes (within the error bars) for lattice dimensions $d = 1, 2, 3$; on the other hand, its dependence on both α and U is analyzed in detail. In the next section we define the α -XY model, reviewing some results of previous works. In Sec. III we present our numerical analysis, carried through molecular-dynamics simulations, leading to the scaling in Eq. (1.2). Then, in Sec. IV, we summarize our conclusions.

II. THE INERTIAL α -XY MODEL: SOME PROPERTIES OF QUASI-STATIONARY STATES

The fully coupled HMF model has been extended to a long-range-interaction model, where two-body interactions decay with the distance r_{ij} as $1/r_{ij}^\alpha$ ($\alpha \geq 0$), the so-called α -XY inertial model, defined by the Hamiltonian [21]

$$\mathcal{H} = K + V_\alpha = \sum_{i=1}^N E_i, \quad (2.1)$$

$$E_i = \frac{p_i^2}{2} + \frac{1}{2\tilde{N}} \sum_{j \neq i}^N \frac{1 - \cos(\theta_i - \theta_j)}{r_{ij}^\alpha}. \quad (2.1)$$

From now on, without loss of generality, we set moments of inertia, coupling constants, as well as k_B , equal to unity. The two time-dependent contributions, $K \equiv K(t)$ and $V_\alpha \equiv V_\alpha(t)$, represent the kinetic and potential energies at time t , whereas $E_i \equiv E_i(t)$ stand for one-particle energies; these quantities follow the conservation of total energy, i.e., $\mathcal{H} = K(t) + V_\alpha(t) = \sum_i E_i(t) = \text{const} (\forall t)$. Hence, the model consists of N two-component rotators (with length normalized to unity), located at the sites of a d -dimensional hypercubic lattice of linear size L ($N \equiv L^d$) and the ferromagnetic interactions between pairs decay with their respective distance $r_{ij} = |\mathbf{r}_i - \mathbf{r}_j|$ (measured in lattice units and defined as the minimal one, since periodic conditions are used). The interaction range is controlled by the parameter $\alpha \geq 0$, which allows an interpolation between two special limits, namely, $\alpha = 0$ (HMF model) and $\alpha \rightarrow \infty$ (ferromagnetic nearest-neighbor-interaction model in d dimensions). Furthermore, the prefactor in the potential energy of Hamiltonian (2.1) yields an ‘‘extensive’’ energy for all values of α/d , where [22,23]

$$\tilde{N} = \frac{1}{N} \sum_{i=1}^N \sum_{j \neq i}^N \frac{1}{r_{ij}^\alpha} = \sum_{j=2}^N \frac{1}{r_{1j}^\alpha}, \quad (2.2)$$

recovering the expected quantities in the two special limits, i.e., $\tilde{N} = N - 1 \sim N$ ($\alpha = 0$) and $\tilde{N} = 2d$ ($\alpha \rightarrow \infty$).

A relevant characteristic of the model defined in Eq. (2.1) concerns the fact that its time evolution can be followed numerically through molecular-dynamics simulations, i.e., by a direct integration of the equations of motion,

$$\dot{\theta}_i = \frac{\partial \mathcal{H}}{\partial p_i} = p_i, \quad \dot{p}_i = -\frac{\partial \mathcal{H}}{\partial \theta_i} = -\frac{1}{\tilde{N}} \sum_{j \neq i}^N \frac{\sin(\theta_i - \theta_j)}{r_{ij}^\alpha}, \quad (2.3)$$

where the angle $\theta_i(t)$, together with its conjugated angular momentum $p_i(t)$, describe the state of rotator i ($i = 1, 2, \dots, N$)

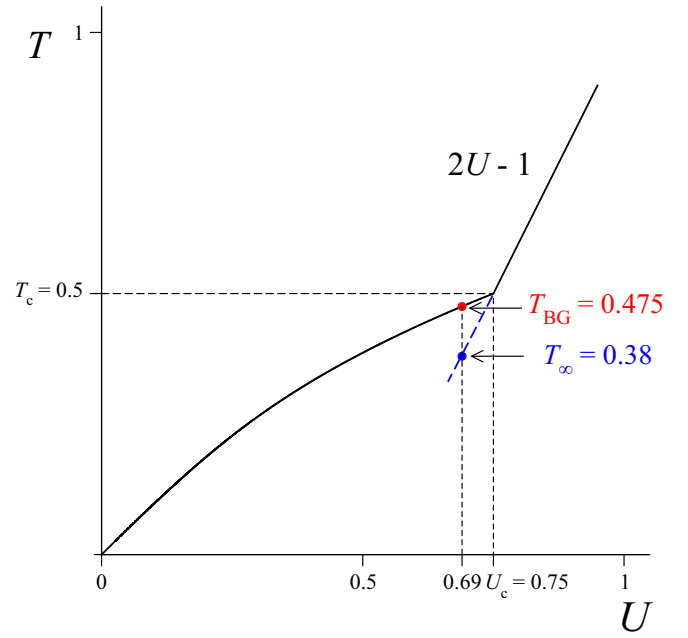


FIG. 1. The caloric curve of the α -XY model [cf. Eq. (2.6)] applies to the whole long-range-interaction regime ($0 \leq \alpha/d \leq 1$), and exhibits a ferromagnetic-paramagnetic continuous phase transition at the critical values $T_c = 1/2$ and $U_c = 3/4$. The blue dashed line in the ferromagnetic phase ($U \lesssim U_c$) represents the set of kinetic temperatures T_∞ , associated with the QSSs in the limit $N \rightarrow \infty$ [cf. Eq. (1.1)]. By monitoring numerically the time evolution of the average kinetic temperature $T(t)$, one finds a plateau associated with T_∞ , followed by a later state whose temperature T_{BG} ($T_{BG} > T_\infty$) coincides with the one predicted by BG statistical mechanics; these two temperatures are illustrated for an energy per particle $U = 0.69$.

at time t . Two important quantities, namely, the kinetic temperature and internal energy per particle, can be defined in the usual way,

$$T(t) \equiv \frac{2}{N} \langle K(t) \rangle, \quad U \equiv \frac{\langle \mathcal{H} \rangle}{N} = \frac{1}{N} \sum_i \langle E_i(t) \rangle, \quad (2.4)$$

whereas a ferromagnetic order (whenever present) is characterized by the norm of the magnetization vector,

$$\vec{M}(t) = \frac{1}{N} \sum_{i=1}^N \vec{S}_i(t), \quad (2.5)$$

with $\vec{S}_i(t) \equiv [\cos \theta_i(t), \sin \theta_i(t)]$. In the HMF limit ($\alpha = 0$) one gets from Eq. (2.1),

$$U = \frac{T}{2} + \frac{1}{2}(1 - M^2), \quad (2.6)$$

leading to a ferromagnetic-paramagnetic continuous phase transition at the critical values $T_c = 1/2$ and $U_c = 3/4$ (see Fig. 1).

The α -XY model has been studied either on a ring (dimension $d = 1$) (see, e.g., Refs. [21,24–26]), or on d -dimensional lattices ($d = 1, 2, 3$) [27–30]. By monitoring the range of the interactions, these analyses identified two distinct regimes, namely, a long-range- ($0 \leq \alpha/d \leq 1$) and short-range-interaction ($\alpha/d > 1$) one, as described next.

Throughout the long-range regime, most properties of the HMF limit continue to be valid, e.g., the expression for the internal energy in Eq. (2.6), and consequently, the ferromagnetic-paramagnetic phase transition at the critical values $T_c = 1/2$ and $U_c = 3/4$ [24,25]. The caloric curve of the α -XY model is shown in Fig. 1, where the blue dashed line represents a low-temperature extension of the paramagnetic branch, similar to what is observed in supercooled liquids [19,20]. For values of the energy per particle below (but close) to the critical value ($U \lesssim U_c$), numerical analyses of the time evolution of the average kinetic temperature $T(t)$ usually find a QSS, characterized by a kinetic temperature T_∞ [cf. Eq. (1.1)], followed by a later state with a temperature T_{BG} ($T_{BG} > T_\infty$). These two distinct kinetic temperatures that occur in the ferromagnetic phase (as illustrated in Fig. 1 for an energy per particle $U = 0.69$) appear as a consequence of the QSS, which is expected to be influenced by strong correlations near criticality. Indeed, the QSS disappears at the critical point, so that one finds that $(T_{BG} - T_\infty) \rightarrow 0$ as $U \rightarrow U_c$, leading to $T_{BG} = T_\infty = 1/2$ at $U = U_c$. Moreover, throughout the whole paramagnetic phase, i.e., for $U > U_c$, there is no difference between these two temperatures, and consequently, no QSS. On the other hand, along the short-range regime there is no QSS, and the dimension d starts playing a significant role, as expected, leading to distinct properties for various d [27–30]. Particularly, it was shown that the largest Lyapunov exponent scales with the total number of rotators as $N^{-\kappa}$, where κ depends on (α, d) only through the ratio α/d , leading to $\kappa > 0$ in the long-range regime, whereas $\kappa \rightarrow 0$ in the short-range regime, corresponding to positive Lyapunov exponents.

Many features of the α -XY model, in its long-range-interaction regime, have been appropriately described within nonextensive statistical mechanics [5,6]. This framework emerged through the proposal of a generalized entropic form [31],

$$S_q = k \sum_{i=1}^w p_i \left(\ln_q \frac{1}{p_i} \right), \quad (2.7)$$

where

$$\ln_q u \equiv (u^{1-q} - 1)/(1 - q) \quad (\ln_1 u = \ln u), \quad (2.8)$$

which is characterized by an index q ($q \in \mathbb{R}$), recovering BG entropy in the limit $q \rightarrow 1$, i.e., $S_1 \equiv S_{BG}$. Consequently, the distributions that optimize the entropy S_q generalize the Gaussian into the usually referred to as q -Gaussian probability distributions [5,6]. These probability distributions have been obtained for the time-averaged momenta distributions, both before and after the transition to the long-standing state whose kinetic temperature T_{BG} coincides with that of the BG equilibrium state, with a value of the entropic index $q = q_p(\alpha/d)$ within the long-range regime [28]. On the other hand, Maxwellian distributions were found in the limiting short-range regime, as well as for ensemble-averaged momenta probability distributions. Deviations from BG predictions have also been observed for time-averaged energy probability distributions, where instead of the BG exponential, q -exponential probability distributions emerged from the simulations in the long-range regime, with $q = q_E(\alpha/d)$ [28].

Similar results have been obtained in a long-range-interaction Fermi-Pasta-Ulam model [32–36], as well as for a model analogous to the one in Eq. (2.1), defined in terms of Heisenberg (three-component) classical rotators [37–39]. This latter system, usually called the inertial α -Heisenberg model, exhibits QSSs throughout its whole long-range-interaction regime ($0 \leq \alpha/d \leq 1$), for $U \lesssim U_c$ (where $U_c = 5/6$ for Heisenberg rotators). Recent detailed numerical analyses focused on the duration t_{QSS} of these QSSs, for both α -XY [29,30] and α -Heisenberg [39] inertial models. It was shown that t_{QSS} presents qualitatively similar behavior for these two models, i.e., it depends on N , α , and d , although the dependence on α appears only through the ratio α/d . In fact, t_{QSS} decreases with α/d and increases with both N and d [29,39]. Numerical data are displayed in Fig. 2, for the α -XY model in dimensions $d = 1, 2, 3$ and typical values of the energy per particle, where we exhibit the growth of t_{QSS} with N for $\alpha/d = 0.9$ [Fig. 2(a)], as well as its decrease with α/d for $N = 46\,656$ [Fig. 2(b)]. The plots of Fig. 2(a) indicate that [29]

$$t_{QSS} = d^\rho \mu(\alpha/d) N^{A(\alpha/d)}, \quad (2.9)$$

whereas those of Fig. 2(b) yield

$$t_{QSS} = d^\rho v(N) \exp[-B(N)(\alpha/d)^2], \quad (2.10)$$

with the exponent $A(\alpha/d)$ [$A(\alpha/d) \simeq 1.77 - 0.73(\alpha/d)^2 - 1.02(\alpha/d)^4$], as well as the coefficient $B(N)$ [$B(N) \simeq N^{0.21}$], remaining independent of U (within error bars), i.e., $A(0.9) = 0.52 \pm 0.02$ and $B(46\,656) = 9.40 \pm 0.12$. It should be mentioned that the data presented in Fig. 2 lead to Eqs. (2.9) and (2.10) independent of a particular choice for the total energy per particle (within error bars), extending the results of Ref. [29], which focused on $U = 0.69$; this remains valid as far as the values of U are sufficiently below the critical value U_c . Indeed, an investigation of the limit $U \rightarrow U_c$ for the α -XY model [30] showed that the duration t_{QSS} goes through a critical phenomenon, namely $t_{QSS} \propto (U_c - U)^{-\xi}$, and universality was found for the critical exponent $\xi \simeq 5/3$, throughout the whole long-range-interaction regime.

Besides the duration t_{QSS} , another important quantity characterizes these QSSs, namely, its kinetic temperature $T_{QSS}(N, \alpha, d)$. In the next section we will give special attention to this latter quantity for the α -XY model, approaching the limit $N \rightarrow \infty$ [cf. Eq. (1.1)] through the scaling proposed in Eq. (1.2).

III. NUMERICAL RESULTS FOR T_{QSS}

We are going to probe values of $U < U_c$, although avoiding the limit $U \rightarrow U_c$, since one expects that the critical phenomenon related to the duration t_{QSS} [30] may influence the behavior of T_{QSS} . Therefore, we will consider three values for the total energy per particle, more specifically, $U = 0.69$ (which has been widely used in the literature for the HMF and α -XY models), in addition to $U = 0.65$ and $U = 0.72$. The results that follow were obtained by applying the same numerical procedure used in Refs. [29,30], i.e., the $2N$ equations in (2.3) were integrated by means of a fourth-order symplectic algorithm [40], considering an integration step $h = 0.2$, yielding conservation of the

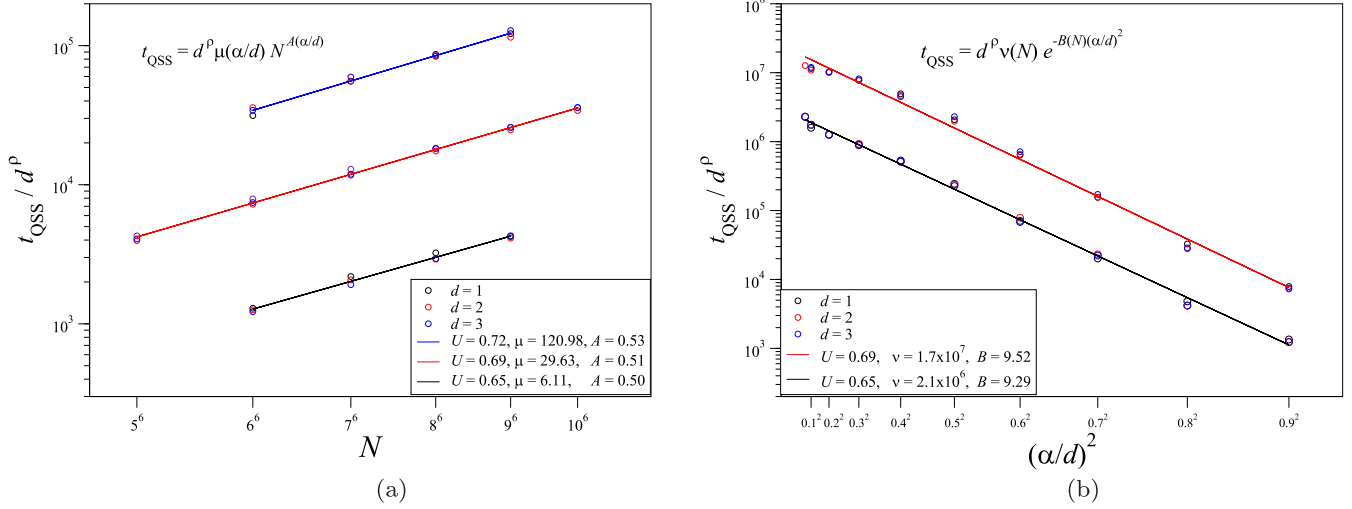


FIG. 2. (a) The durations of the QSSs for the α -XY model $\alpha/d = 0.9$ are represented conveniently vs the total number of rotators in a log-log scale, showing numerical data for $N = l^6$ ($l = 5, 6, 7, 8, 9, 10$), dimensions $d = 1, 2, 3$, and typical values of the energy per particle (decreasing values of U from top to bottom). Straight-line fittings lead to the scaling of Eq. (2.9), where $A(0.9) = 0.52 \pm 0.02$. (b) The durations of the QSSs for the α -XY model ($N = 6^6 = 46\,656$) are exhibited vs $(\alpha/d)^2$ ($0 \leq \alpha/d \leq 0.9$) in a log-linear scale, for $d = 1, 2, 3$, and two typical values of the energy per particle: $U = 0.69$ (upper straight line) and $U = 0.65$ (lower straight line); the straight-line fittings follow the scaling of Eq. (2.10), where $B(46\,656) = 9.40 \pm 0.12$. In both panels, data were obtained considering the initial condition $M(0) \simeq 0$; the factor d^ρ becomes important as one approaches the short-range-interaction threshold, so that $\rho = 0$ ($\alpha/d \leq 0.7$) and $\rho = 0.31$ ($\alpha/d = 0.8, 0.9$), and one expects that $\rho \rightarrow 0$ in the thermodynamic limit, for all $0 \leq \alpha/d \leq 1$ [29]. For the values of U considered, the exponent $A(\alpha/d)$ [Eq. (2.9)], as well as the coefficient $B(N)$ [Eq. (2.10)], are essentially independent of U , within error bars.

energy per particle within a relative precision of 10^{-4} (at least) throughout all our calculations. Moreover, we applied periodic boundary conditions and a fast-Fourier-transform algorithm, for which the total number of rotators were chosen as $N = l^6 = (l^3)^2 = (l^2)^3$ ($l = 5, 6, 7, 8, 9, 10$), all of them being expressed in the form $N = L^d$ ($d = 1, 2, 3$). Hence, we used $N = 15\,625 = (125)^2 = (25)^3$, $46\,656 = (216)^2 = (36)^3$, $117\,649 = (343)^2 = (49)^3$, $262\,144 = (512)^2 = (64)^3$, $531\,441 = (729)^2 = (81)^3$, and $10^6 = (1000)^2 = (100)^3$. At the initial time, the angular momenta $\{p_i\}$ were drawn from a uniform distribution, $p_i \in [-1, 1]$, then rescaled to achieve the desired value for U and $\sum_i p_i = 0$. For the angles, we chose θ_i from a uniform distribution $\theta_i \in [0, 2\pi]$, corresponding to minimum $[M(0) \simeq 0]$ total magnetization. As the analyses of Refs. [29,30] concerning the duration t_{QSS} , simulations using the initial condition $\theta_i = 0$ ($\forall i$), corresponding to maximum $[M(0) = 1]$ total magnetization, are expected to yield similar results (within error bars).

In Fig. 3 we present numerical results obtained from simulations of the inertial α -XY model in a closed ring ($d = 1$), $\alpha = 0.9$, and total energy per rotator $U = 0.69$. In Fig. 3(a) we exhibit the time evolution of the total magnetization squared $M^2(t)$, together with the difference $T(t) - T_\infty$, in a linear-log plot for a total number of rotators $N = 6^6 = 46\,656$. Although the data shown for the QSS present essentially $M(t) \simeq 0$, the equation of state [cf. Eq. (2.6)] does not agree with Eq. (1.1), namely, $T_\infty \equiv 2U - 1$. These results indicate that finite-size effects are clearly playing a significant role in such a violation, indicating that the paramagnetic branch of Eq. (2.6) should converge to Eq. (1.1) only in the limit $N \rightarrow \infty$. This result is reinforced in Fig. 3(b), where we

show the time evolution of the kinetic temperature $T(t)$ for an increasing number of rotators, $N = l^6$ ($l = 5, 6, 7, 8, 9, 10$), and one notices a clear convergence to the limit of Eq. (1.1) in the respective inset.

The kinetic temperatures $T(t)$ of the inertial α -XY model (total energy per rotator $U = 0.69$) are exhibited versus time in Fig. 4, for typical values of (N, α, d) . In Fig. 4(a) we plot data for a total number of rotators $N = 6^6 = 46\,656$ along a closed ring ($d = 1$) and several values of α ($0 \leq \alpha \leq 1$), showing that T_{QSS} grows with α , as illustrated in the lower inset, where the associated differences $T_{\text{QSS}} - T_\infty$ are represented versus α . The results of Fig. 4(b) [total number of rotators $N = 10^6$, $\alpha/d = 0.9$, and dimensions $d = 1, 2, 3$] reinforce that the duration t_{QSS} grows with d , as already shown in Ref. [29]. Moreover, one notices that the associated temperatures T_{QSS} are slightly dependent on d , decreasing as d increases. Comparing the results of Figs. 4(a) and 4(b), one obtains that T_{QSS} is more sensible to changes in α , than to those in d . In fact, by estimating the relative discrepancy, $(T_{\text{QSS}} - T_\infty)/T_\infty$, one concludes that such a quantity may be of the order 6–8 times larger in cases of Fig. 4(a), when compared to those of Fig. 4(b).

In Fig. 5 we analyze the scaling proposed in Eq. (1.2) by plotting the difference $T_{\text{QSS}} - T_\infty$ vs N in log-linear representations. This is carried for typical values of α ($0 \leq \alpha \leq 1$), dimensions $d = 1, 2, 3$, and three different values of the energy per particle [cf. Figs. 5(a)–5(c)]. As discussed in Fig. 4, the values of T_{QSS} are more sensible to changes in α than to those in d ; consistently, in Fig. 5(d) similar studies are restricted to dimension $d = 1$. In all cases considered, the scaling proposed in Eq. (1.2) is verified, allowing us to

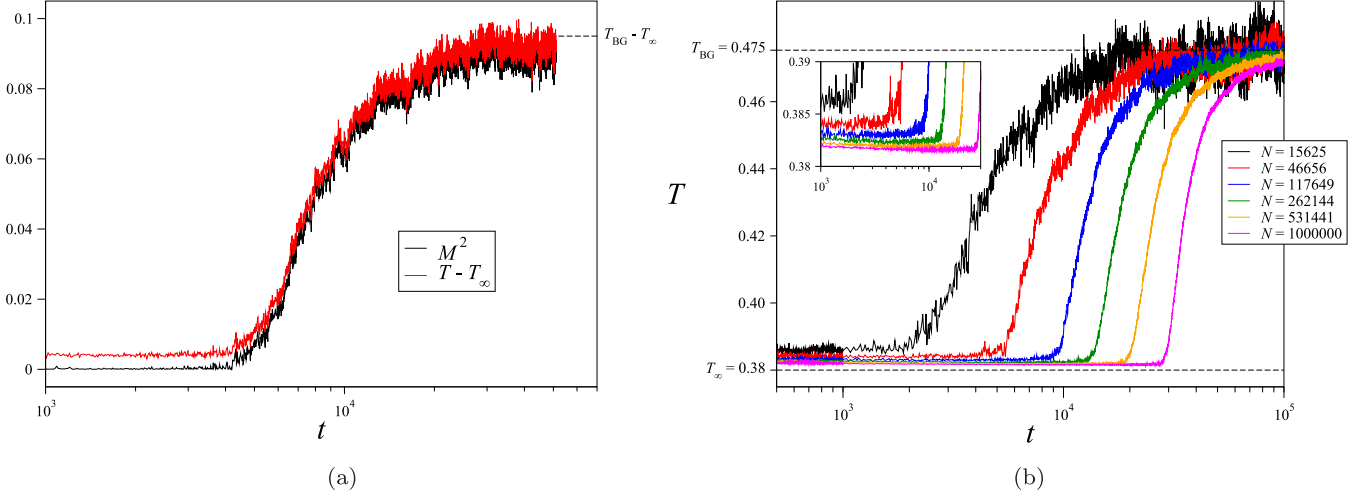


FIG. 3. Numerical data obtained from simulations of the inertial α -XY model in a closed ring ($d = 1$), $\alpha = 0.9$, total energy per rotator $U = 0.69$, and an initial total magnetization $M(0) \simeq 0$, are represented vs time in linear-log scales. (a) The total magnetization squared $M^2(t)$ (lower black line), as well as the difference of the kinetic temperature with respect to its value in the limit $N \rightarrow \infty$, $T(t) - T_\infty$ (upper red line), are plotted for a total number of rotators $N = 6^6 = 46\,656$. The results show that the agreement of the equation of state [cf. Eq. (2.6)] along its paramagnetic branch ($M = 0$), with $T_\infty \equiv 2U - 1$ [Eq. (1.1)], is strictly valid throughout the QSS only for $N \rightarrow \infty$, but it is slightly violated for finite N . (b) The kinetic temperature $T(t)$ is plotted for different number of rotators, $N = l^6$ ($l = 5, 6, 7, 8, 9, 10$); the inset on the left displays an enlargement of a time window illustrating the limit of Eq. (1.1). According to Fig. 1, the associated characteristic temperatures are $T_\infty = 0.38$ and $T_{BG} = 0.475$.

compute the exponent β , and the results are plotted in the lower insets (β vs α); as expected, the estimates do not vary (within error bars) for different dimensions. These plots indicate that β remains essentially unchanged (close to unity) for smaller values of α , i.e., $\beta = 0.94 \pm 0.07$ ($0 \leq \alpha \leq 0.5$), whereas it typically decays linearly for $\alpha > 0.5$. One expects that $\beta \rightarrow 0$ as $\alpha/d \rightarrow 1$, remaining zero throughout the

whole short-range regime ($\alpha/d > 1$), since the QSS should disappear for $\alpha/d \geq 1$. However, as verified in previous investigations (see, e.g., Refs. [28–30]), the crossover from the long-range-interaction regime ($0 \leq \alpha/d \leq 1$) to the short-range one ($\alpha/d > 1$) is characterized by strong finite-size effects, which are also expected to play an important role in the present analysis. This explains the numerical results for

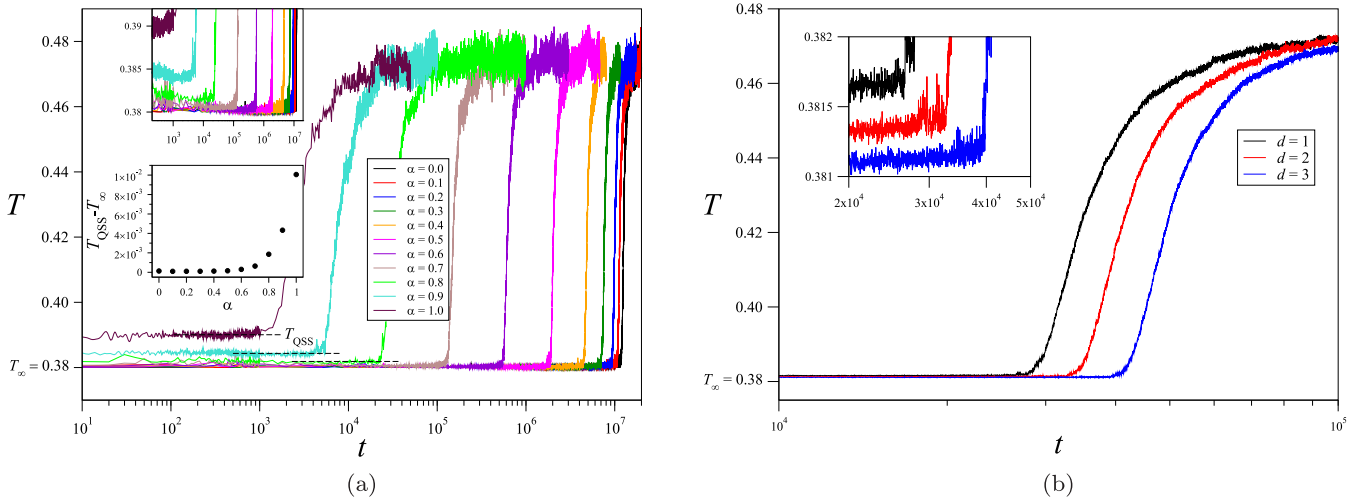


FIG. 4. The kinetic temperature $T(t)$ is represented vs time in linear-log plots, for the inertial α -XY model with an energy per rotator $U = 0.69$ and initial magnetization $M(0) \simeq 0$. (a) Data for a total number of rotators $N = 6^6 = 46\,656$ along a closed ring ($d = 1$) and several values of α ($0 \leq \alpha \leq 1$). In the upper inset we show a time window highlighting the changes from the QSSs to the second plateau in linear-log plots, emphasizing the increase of T_{QSS} with α ; the corresponding differences $T_{QSS} - T_\infty$ are represented vs α in the lower inset. (b) Data for a total number of rotators $N = 10^6$, $\alpha/d = 0.9$, and dimensions $d = 1, 2, 3$, showing that the duration t_{QSS} increases with d [29]. The changes from the QSSs to the second plateau are highlighted in the inset in a linear-log plot, showing that T_{QSS} presents a slight dependence on d , i.e., decreasing as d increases. Throughout the whole long-range regime ($0 \leq \alpha/d \leq 1$), the corresponding characteristic temperatures are $T_\infty = 0.38$ and $T_{BG} = 0.475$.

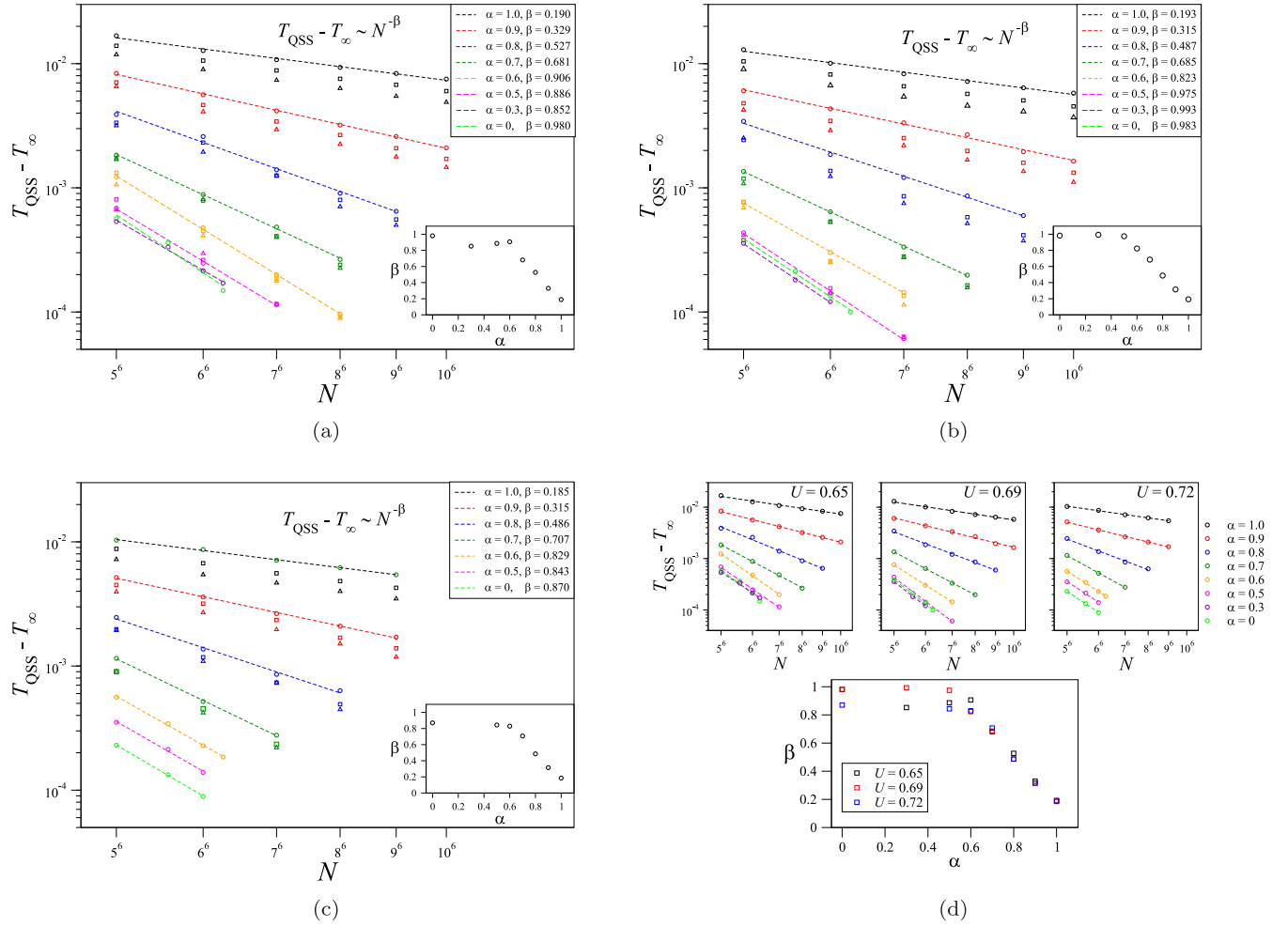


FIG. 5. The differences $T_{\text{QSS}} - T_{\infty}$ are represented vs N (*log-log scales*) for the inertial α -XY model, considering typical values of α ($0 \leq \alpha \leq 1$), dimensions $d = 1$ (circles), $d = 2$ (squares), and $d = 3$ (triangles), initial magnetization $M(0) \simeq 0$, and different values of the total energy per particle: (a) $U = 0.65$; (b) $U = 0.69$; (c) $U = 0.72$. Let us emphasize that the data for T_{QSS} are more sensible to changes in α , than to those in d , as pointed out in Fig. 4; due to this, in (d) similar analyses are carried only for $d = 1$. By considering the scaling of Eq. (1.2), the corresponding values for the exponent β are estimated in each case, and the results are plotted in the lower insets (β vs α). In all cases considered, one notices that $T_{\text{QSS}} \rightarrow T_{\infty}$ as $N \rightarrow \infty$ [following Eq. (1.2)], and the exponent β essentially remains unchanged (within numerical error bars) for ($0 \leq \alpha \leq 0.5$) and appears to decay linearly for $0.5 < \alpha \leq 1.0$.

$\alpha = 1$ (in all cases shown in Fig. 5), where small positive values of β are found.

The data for the temperature T_{QSS} presented herein can also be treated appropriately to produce collapsed curves for each energy value, dimensions $d = 1, 2, 3$, and different values of α , similarly to what was done for the duration t_{QSS} [29]. This is illustrated in Fig. 6, where we present data from Fig. 5(b) (total energy per particle $U = 0.69$ and dimensions $d = 1, 2, 3$); these data are collapsed for each value of α by introducing a multiplicative factor $f(\alpha, d)$ in the ordinate (see inset). As one approaches the short-range-interaction threshold (e.g., $\alpha/d = 0.9$) this factor recovers $f(d) = d^{-\rho}$, used in Ref. [29] for the analyses of the duration t_{QSS} , where $\rho = 0.35 \pm 0.04$ is in agreement with the previous results within error bars.

IV. CONCLUSIONS

The longstanding quasi-stationary states of the d -dimensional classical inertial α -XY ferromagnet, with two-

body interactions decaying as $1/r_{ij}^{\alpha}$ ($\alpha \geq 0$), were investigated numerically through first-principles microcanonical molecular-dynamics simulations. This model consists of N two-component rotators, located at the sites of a d -dimensional hypercubic lattice of linear size L ($N \equiv L^d$), which are characterized by two distinct regimes, namely, a long-range- ($0 \leq \alpha/d \leq 1$) and a short-range-interaction ($\alpha/d > 1$) one. Throughout the first regime, most properties of the $\alpha = 0$ limit continue to be valid, e.g., a ferromagnetic-paramagnetic phase transition at the critical values for the total energy per particle and associated temperature ($U_c = 3/4$, $T_c = 1/2$). Along the paramagnetic phase these thermodynamic quantities follow a simple linear relation, i.e., $T = 2U - 1$.

Two important quantities characterize these quasi-stationary states, namely, their duration $t_{\text{QSS}}(N, \alpha, d)$ and kinetic temperature $T_{\text{QSS}}(N, \alpha, d)$. The first one was investigated in detail in previous works: (i) In Ref. [29], by concentrating on a particular value of total energy per particle

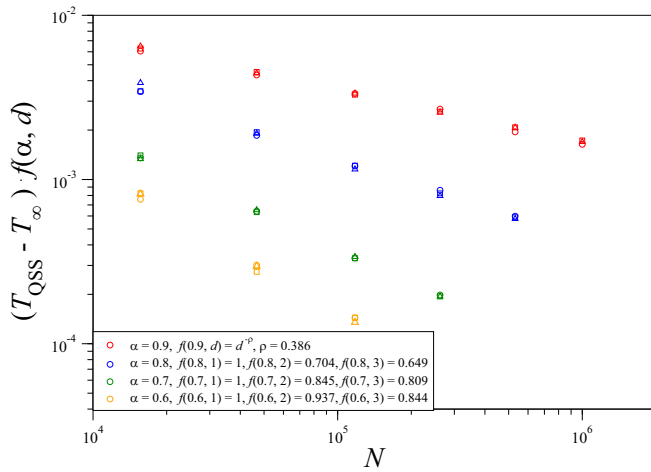


FIG. 6. Data from Fig. 5(b) (total energy per particle $U = 0.69$ and dimensions $d = 1, 2, 3$) are collapsed for each value of α ($\alpha = 0.6, 0.7, 0.8, 0.9$ from bottom to top) by introducing a factor $f(\alpha, d)$ in the ordinate (see inset). As one approaches the short-range-interaction threshold (e.g., $\alpha/d = 0.9$) this factor recovers $f(d) = d^{-\rho}$, used in Ref. [29] for the analyses of the duration t_{QSS} .

($U = 0.69$), it was shown that $t_{\text{QSS}}(N, \alpha, d)$ depends on α only through the ratio α/d . In fact, t_{QSS} decreases with α/d and increases with both N and d . (ii) By focusing on the limit $U \rightarrow U_c$, it was verified that t_{QSS} goes through a critical phenomenon, namely $t_{\text{QSS}} \propto (U_c - U)^{-\xi}$, and universality was found for the critical exponent $\xi \simeq 5/3$, throughout the whole long-range-interaction regime [30]. Herein, we extended the results of Ref. [29], by showing that the general behavior of t_{QSS} essentially does not depend on U , for values of U sufficiently below the critical value $U_c = 3/4$,

i.e., relatively far from the criticality associated with t_{QSS} .

It is known that these quasi-stationary states appear for $U \lesssim U_c$, as a low-temperature extension of the high-temperature (paramagnetic) branch of the caloric curve, although $T_{\text{QSS}}(N, \alpha, d)$ does not match precisely with such an expectation for finite N . Accordingly, the kinetic temperature $T_{\text{QSS}}(N, \alpha, d)$ should approach the limit $T_\infty \equiv 2U - 1$, as $N \rightarrow \infty$, for different values of (α, d) throughout the long-range-interaction regime. Therefore, in the present investigation we focused on T_{QSS} , by proposing (and verifying numerically) the scaling $T_{\text{QSS}} - T_\infty \propto N^{-\beta}$. It was shown that the exponent β essentially does not depend on the choices for U and d ($d = 1, 2, 3$) for fixed α/d ; moreover, it varies with α/d in a simple way, remaining essentially unchanged, i.e., $\beta(\alpha/d) \simeq 1$ for $0 \leq \alpha/d \leq 0.5$, decaying linearly for $\alpha/d > 0.5$, suggesting that $\beta(\alpha/d) \rightarrow 0$ as $\alpha/d \rightarrow 1$.

The present results should be useful for other long-range-interaction systems, such as the inertial α -Heisenberg model, defined in terms of three-component rotators, as well as to some of the most intriguing systems of nature, such as those characterized by gravitational and Coulomb forces. Moreover, since these curious states present similarities with metastable states commonly observed in supercooled liquids, the understanding of their relevant properties, such as their duration and associated temperature, should be relevant also to supercooling phenomena.

ACKNOWLEDGMENT

We have benefited from partial financial support by the Brazilian agencies CNPq and Faperj, and Universidad Politécnic de Madrid.

- [1] R. Balian, *From Microphysics to Macrophysics*, Vols. I and II (Springer, Berlin, 1991).
- [2] L. E. Reichl, *A Modern Course in Statistical Physics*, 2nd edition (Wiley, New York, 1998).
- [3] M. Le Bellac, F. Mortessagne, and G. Batrouni, *Equilibrium and Non-Equilibrium Statistical Thermodynamics* (Cambridge University Press, Cambridge, UK, 2004).
- [4] V. Balakrishnan, *Elements of Nonequilibrium Statistical Mechanics* (CRC Press/Taylor and Francis Group, New York, 2008).
- [5] C. Tsallis, *Introduction to Nonextensive Statistical Mechanics—Approaching a Complex World* (Springer, New York, 2009).
- [6] C. Tsallis, Beyond Boltzmann-Gibbs-Shannon in physics and elsewhere, *Entropy* **21**, 696 (2019).
- [7] M. Antoni and S. Ruffo, Clustering and relaxation in Hamiltonian long-range dynamics, *Phys. Rev. E* **52**, 2361 (1995).
- [8] M.-C. Firpo, Analytic estimation of the Lyapunov exponent in a mean-field model undergoing a phase transition, *Phys. Rev. E* **57**, 6599 (1998).
- [9] V. Latora, A. Rapisarda, and S. Ruffo, Lyapunov Instability and Finite Size Effects in a System with Long-Range Forces, *Phys. Rev. Lett.* **80**, 692 (1998).
- [10] V. Latora, A. Rapisarda, and S. Ruffo, Superdiffusion and Out-of-Equilibrium Chaotic Dynamics with Many Degrees of Freedom, *Phys. Rev. Lett.* **83**, 2104 (1999).
- [11] V. Latora, A. Rapisarda, and C. Tsallis, Non-Gaussian equilibrium in a long-range Hamiltonian system, *Phys. Rev. E* **64**, 056134 (2001).
- [12] J. Barré, F. Bouchet, T. Dauxois, and S. Ruffo, Out-of-Equilibrium States and Statistical Equilibria of an Effective Dynamics in a System with Long-range Interactions, *Phys. Rev. Lett.* **89**, 110601 (2002).
- [13] A. Pluchino, V. Latora, and A. Rapisarda, Metastable states, anomalous distributions and correlations in the HMF model, *Physica D* **193**, 315 (2004).
- [14] A. Pluchino, V. Latora, and A. Rapisarda, Glassy phase in the Hamiltonian mean-field model, *Phys. Rev. E* **69**, 056113 (2004).
- [15] A. Pluchino, V. Latora, and A. Rapisarda, Effective spin-glass Hamiltonian for the anomalous dynamics of the HMF model, *Physica A* **370**, 573 (2006).
- [16] L. G. Moyano and C. Anteneodo, Diffusive anomalies in a long-range Hamiltonian system, *Phys. Rev. E* **74**, 021118 (2006).

- [17] A. Pluchino, A. Rapisarda, and C. Tsallis, Nonergodicity and central-limit behavior for long-range Hamiltonians, *Europhys. Lett.* **80**, 26002 (2007).
- [18] A. Pluchino, A. Rapisarda, and C. Tsallis, A closer look at the indications of q -generalized Central Limit Theorem behavior in quasi-stationary states of the HMF model, *Physica A* **387**, 3121 (2008).
- [19] P. G. Debenedetti, *Metastable Liquids: Concepts and Principles* (Princeton University Press, Princeton, NJ, 1996).
- [20] S. P. Das, *Statistical Physics of Liquids at Freezing and Beyond* (Cambridge University Press, Cambridge, UK, 2011).
- [21] C. Anteneodo and C. Tsallis, Breakdown of Exponential Sensitivity to Initial Conditions: Role of the Range of Interactions, *Phys. Rev. Lett.* **80**, 5313 (1998).
- [22] P. Jund, S. G. Kim, and C. Tsallis, Crossover from extensive to nonextensive behavior driven by long-range interactions, *Phys. Rev. B* **52**, 50 (1995).
- [23] C. Tsallis, Nonextensive thermostatics and fractals, *Fractals* **3**, 541 (1995).
- [24] A. Campa, A. Giansanti, and D. Moroni, Canonical solution of a system of long-range interacting rotators on a lattice, *Phys. Rev. E* **62**, 303 (2000).
- [25] F. Tamarit and C. Anteneodo, Rotators with Long-range Interactions: Connection with the Mean-Field Approximation, *Phys. Rev. Lett.* **84**, 208 (2000).
- [26] A. Campa, A. Giansanti, D. Moroni, and C. Tsallis, Classical spin systems with long-range interactions: universal reduction of mixing, *Phys. Lett. A* **286**, 251 (2001).
- [27] L. J. L. Cirto, V. R. V. Assis, and C. Tsallis, Influence of the interaction range on the thermostatics of a classical many-body system, *Physica A* **393**, 286 (2014).
- [28] L. J. L. Cirto, A. Rodríguez, F. D. Nobre, and C. Tsallis, Validity and failure of the Boltzmann weight, *Europhys. Lett.* **123**, 30003 (2018).
- [29] A. Rodríguez, F. D. Nobre, and C. Tsallis, Quasi-stationary-state duration in the classical d -dimensional long-range inertial XY ferromagnet, *Phys. Rev. E* **103**, 042110 (2021).
- [30] A. Rodríguez, F. D. Nobre, and C. Tsallis, Criticality in the duration of quasistationary state, *Phys. Rev. E* **104**, 014144 (2021).
- [31] C. Tsallis, Possible generalization of Boltzmann-Gibbs statistics, *J. Stat. Phys.* **52**, 479 (1988).
- [32] C. G. Antonopoulos and H. Christodoulidi, Weak chaos detection in the Fermi-Pasta-Ulam- α system using q -Gaussian statistics, *Int. J. Bifurcation Chaos Appl. Sci. Eng.* **21**, 2285 (2011).
- [33] H. Christodoulidi, C. Tsallis, and T. Bountis, Fermi-Pasta-Ulam model with long-range interactions: Dynamics and thermostatics, *Europhys. Lett.* **108**, 40006 (2014).
- [34] H. Christodoulidi, T. Bountis, C. Tsallis, and L. Drossos, Dynamics and statistics of the Fermi-Pasta-Ulam β -model with different ranges of particle interactions, *J. Stat. Mech.-Theory Exp.* (2016) 123206.
- [35] D. Bagchi and C. Tsallis, Sensitivity to initial conditions of a d -dimensional long-range interacting quartic Fermi-Pasta-Ulam model: Universal scaling, *Phys. Rev. E* **93**, 062213 (2016).
- [36] D. Bagchi and C. Tsallis, Fermi-Pasta-Ulam-Tsingou problems: Passage from Boltzmann to q -statistics, *Physica A* **491**, 869 (2018).
- [37] L. J. L. Cirto, L. S. Lima, and F. D. Nobre, Controlling the range of interactions in the classical inertial ferromagnetic Heisenberg model: analysis of metastable states, *J. Stat. Mech.-Theory Exp.* (2015) P04012.
- [38] A. Rodríguez, F. D. Nobre, and C. Tsallis, d -Dimensional classical Heisenberg model with arbitrarily-ranged interactions: Lyapunov exponents and distributions of momenta and energies, *Entropy* **21**, 31 (2019).
- [39] A. Rodríguez, F. D. Nobre, and C. Tsallis, Quasi-stationary-state duration in d -dimensional long-range model, *Phys. Rev. Research* **2**, 023153 (2020).
- [40] H. Yoshida, Construction of higher order symplectic integrators, *Phys. Lett. A* **150**, 262 (1990).